TRANSIENT RESPONSE OF TURBINE FLOW METERS DURING THE APPLICATION AT A HIGH PRESSURE PISTON PROVER

Bodo Mickan, Rainer Kramer, Volker Strunck
Physikalisch Technische Bundesanstalt [PTB]
Bundesallee 100, D-38116 Braunschweig, Germany
Tel: +49 531 592 1330, Fax: +49 531 592 69 1330, e-mail: Bodo.Mickan@ptb.de

Toralf Dietz
SICK MAIHAK GmbH
Bergener Ring 27, D-01458 Ottendorf-Okrilla, Germany
Tel: +49 35205 524 13, Fax: : +49 35205 524 22, e-mail: Toralf.Dietz@sick.de

Abstract: In Germany, a high pressure piston prover has been operated as the national volumetric primary standard for high-pressure natural gas for more than 15 years. The reliability and the claimed uncertainty of this system was proven in international key comparisons in which all relevant physical principles of traceability for gas measurements were assed.
One important part of the uncertainty budget for the volume at the location of the meter under test (MuT) are dynamic effects caused by the limited dynamic in the transient response of the MuT in its indication of the flow. This impact of the limited transient response can be corrected if the volume indication (pulses) of the meter is measured with a high time resolution and if an appropriate model of the transient response for the meter is available.
The paper will describe the results of determination of the system model for a turbine meter and the model parameters. The experimental determination of the system parameters were based on measurements of meter indication as well as flow speed by means of LDV-equipment (at atmospheric conditions) and their verification by means of an ultrasonic-meter (at high pressure). The positive effect on the calibration results with the high pressure piston prover will be demonstrated and discussed.

Keywords: piston prover, mechanical flow meter, turbine meter, transient response, corrected indication, Laser Doppler velocimetry, ultra sonic meter

1. Introduction

It is the common practice of calibration and application of turbine flow meters (and also for other fluid flow meters) to assume a direct time independent relationship between the indicated flow rate $q_{TM,ind}$ and the real flow rate q which can be expressed as a meter factor $K = q_{TM,ind}/q$. But this is only valid under the ideal condition of constant flow rate $q \neq f(t)$. Due to the physical dynamic behaviour of the signal transformation via the turbine wheel to the indication of the meter we have to consider a time variation in the relationship $q_{TM,ind}/q$ what defines a system function $G(t)$ describing the general physical process of signal transformation (see Fig. 1).

In the practise of calibration it is the normal strategy to establish flow rates with very small variations to keep the influence of the dynamic behaviour insignificant compared to the total uncertainty of the calibration process. Secondly, for the application of the meters there are also recommendations or rules to limit this influence, e.g. in the legal metrology in Germany the technical rule TRG 13 [1] which gives measures to ensure correct measurements within the

maximal permissible errors in service depending on size of turbine meters and the flow regime at application. But these rules are rather rough and not applicable to correct a badly influenced indication.

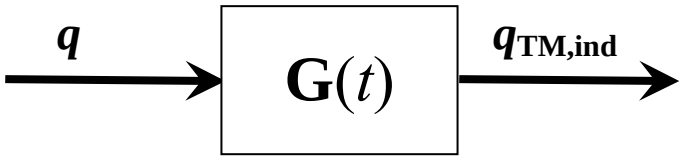

Fig. 1 Relationship of real flow rate q and flow rate $q_{TM,ind}$ indicated by turbine meter via system function G(t)

In comparison to this we like to consider here a situation were the detailed knowledge about the system function G(t) is necessary which is the calibration of turbine meters with a passive piston prover system. It is in the nature of a passive piston prover system that we have variations in the flow passing the meter, especially at the beginning of the calibration run. Due to the very limited time span of the complete calibration run it is not necessarily the case that the flow indication is practically not influenced during the data collection (compared to the needs for uncertainty). Also here it was the old approach to set limits to the allowed variations of flow rate during the calibration run to ensure limited impacts to the total uncertainty of the calibration result [2].

Our new approach for this situation is the detailed determination of the system function $G(t)$ and its application for corrections of the meter indication to remove the influence of flow rate variations. Hence, in the following we describe the development of the mathematical system function $G(t)$ outgoing from the physical relationship of forces and momentums at the turbine wheel, the determination of the model parameter based on measurements in a special experimental setup under atmospheric conditions and finally the verification and application for the calibration of a turbine meter using the high pressure piston prover of PTB.

We like to point out that the principles and methods shown in this paper are applicable to any other mechanical meter type as well as other measurement situations with varying flow rates. Therefore the paper provides a good base for further developments of the wide topic of so called dynamic measurements besides the very specific intention of these investigations here to improve the calibration using the high pressure piston prover.

2. Mathematical model of dynamic response for turbine meters

The basis for the development of the mathematical system function $G(t)$ is a schematic velocity plan as given in Fig. 2 and the general momentum balance as given in eq. (1).

As written in eq. (1), the momentum M_{drive} caused by the forces of fluid flow around the turbine wheel is always in balance with M_{fr} caused by friction forces (especially the bearings) and the inertia of the wheel in combination with the rotational acceleration $J \cdot \dot{\omega}$.

$$M_{drive} - J \cdot \dot{\omega} - M_{fr} = 0 \qquad (1)$$

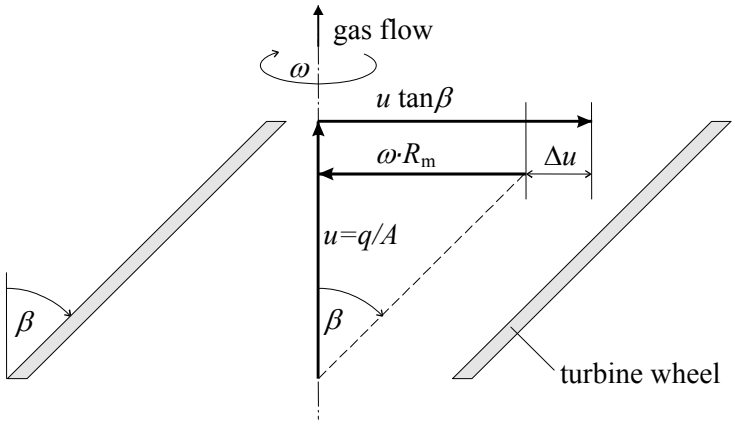

Fig. 2 schematic velocity plan at a turbine wheel

From Fig. 2 we can derive following relations: the wheel is actual rotating with the angular frequency ω which leads to a certain circumferential speed $\omega \cdot R_m$ at a representative mean radius location R_m. At the same time, the fluid flow is passing the turbine wheel in axial direction with the flow velocity u. Based on the inclination angle β of the wheel, the circumferential component of the flow velocity is $u \cdot \tan(\beta)$. The momentum M_{drive} which is accelerating the wheel is then the product of the mass flow rate $\rho \cdot q$, the mean radius R_m and the difference of circumferential component velocity components $\Delta u = u \cdot \tan(\beta) - \omega \cdot R_m$.

$$\rho \cdot q \cdot R_m \cdot \Delta u - J \cdot \dot{\omega} - M_{fr} = 0 \tag{2}$$

The next steps are only some substitutions in eq (2) (see also table 1, list of symbols) and basic transformations.

$$\rho \cdot q \cdot R_m \left(q \frac{\tan \beta}{A} - R_m \cdot \omega \right) - J \cdot \dot{\omega} - M_{fr} = 0 \tag{3}$$

$$c_1 = \rho \frac{R_m}{A} \tan \beta$$
$$c_2 = \rho \cdot R_m^2 \tag{4}$$

$$M_{fr} = M_{fr,0}(\omega_0) + M_{fr,\Delta}(\omega - \omega_0) \tag{5}$$

$$\omega_0 = c_P \cdot q$$
$$\omega = c_P \cdot q_{TM,ind} \tag{6}$$

$$c_1 \cdot q^2 - c_2 \cdot c_P \cdot q \cdot q_{TM,ind} - J \cdot c_P \cdot \dot{q}_{TM,ind} - M_{fr,0}(c_P \cdot q) - M_{fr,\Delta}(c_P [q_{TM,ind} - q]) = 0 \tag{7}$$

Herewith the complete relationship between the real flow rate q and indicated flow rate $q_{TM,ind}$ is given which is dynamic and time depending (include the first derivative of time for the indicated flow rate). For the practical application we need of course more detailed and determinable expressions for the friction caused momentum M_{fr}.

Important for the further steps is the introduction of two parts of the friction caused momentum M_{fr} (see eq. (5)). The first part $M_{fr,0}(\omega_0)$ is specific for the angular frequency ω_0 where ω_0 represent this angular frequency which the wheel would have in the case of stationary conditions ($\dot{\omega}$ =0 or $\dot{q}_{TM,ind}$ =0 rsp.) for the actual given flow speed $u = q/A$. The second part $M_{fr,\Delta}(\omega\text{-}\omega_0)$ gives the additional momentum to $M_{fr,0}$ which is actual present due to the real (instationary) situation with $\omega \neq \omega_0$.

With this definition of the first part $M_{fr,0}(\omega_0)$ we are able to substitute it consequently using the stationary relationship of eq. (7) ($M_{fr,\Delta}(\omega\text{-}\omega_0)$ =0 and $\dot{q}_{TM,ind}$ =0, consider also eq.(6)):

$$c_1 \cdot q^2 - c_2 \cdot c_P \cdot q^2 = M_{fr,0}(c_P \cdot q) \tag{8}$$

which transforms eq. (7) to following:

$$c_2 \cdot c_P \cdot q^2 - c_2 \cdot c_P \cdot q \cdot q_{TM,ind} - J \cdot c_P \cdot \dot{q}_{TM,ind} - M_{fr,\Delta}(c_P[q_{TM,ind} - q]) = 0 \tag{9}$$

It is now necessary to introduce an appropriate expression for the second part of friction based momentum $M_{fr,\Delta}(\omega\text{-}\omega_0)$ to bring it into a relationship to our parameters of interest (q and $q_{TM,ind}$). This is of course empirical and mainly arbitrary it its structure. It was found as a reasonable approach to describe the momentum $M_{fr,\Delta}(\omega\text{-}\omega_0)$ as a proportional relationship to the square of the difference between the real and indicated flow rate as given in eq. (10). The proportionality factor C_{TM} defines a meter specific parameter which has later to be determined in experiments for each individual meter. Please note that other relationships (linear or other combinations with higher orders) were tested but only the quadratic part was found as reasonable and significant.

$$M_{fr,\Delta} = \widetilde{C}_{TM}(c_P[q_{TM,ind} - q])^2 = C_{TM} \cdot c_P(q_{TM,ind} - q)^2 \tag{10}$$

Introduced in eq. (9):

$$c_2 \cdot q^2 - c_2 \cdot q \cdot q_{TM,ind} - J \cdot \dot{q}_{TM,ind} - C_{TM}(q_{TM,ind} - q)^2 = 0 \tag{11}$$

$$(c_2 - C_{TM})q^2 - (c_2 - 2C_{TM})q_{TM,ind} \cdot q - C_{TM} \cdot q_{TM,ind}^2 - J \cdot \dot{q}_{TM,ind} = 0 \tag{12}$$

Eq. (12) is the final solution for the relationship as given in Fig.1, but finally for our intention to find corrections for the meter indication we have to transform it to an explicit equation for the real flow rate in dependency of the indicated flow rate. Fortunately, eq. (12). is a basic quadratic equation which can easily be transformed:

$$q = \frac{1}{2}\left(1 - \frac{C_{TM}}{\rho R_m^2 - C_{TM}}\right)q_{TM,ind} + \sqrt{\frac{1}{4}\left(1 + \frac{C_{TM}}{\rho R_m^2 - C_{TM}}\right)^2 q_{TM,ind}^2 + \frac{J}{\rho R_m^2 - C_{TM}}\dot{q}_{TM,ind}} \tag{13}$$

This result is quit good applicable as far as we have a good knowledge about the meter specific constants J (inertia of the wheel) and C_{TM}[1] as well as a sufficient quality of the first derivative of the indicated flow rate with respect to the time. The last is a question of sampling of the high frequency output and an appropriate signal filtering which is an own topic and not discussed here. For a detailed discussion of this matter one may refer to [3].

3. Determination of model parameters at low pressure

From the basic approach, the determination of the meter specific parameters in eq. (13) is quite simple: you have to establish a flow with well known time dependency, to determine the corresponding meter output signal and to find finally the best fitting values for the parameters in eq. (13). In practise especially the first task is not so easy and need normally the application of a flow rate measurement which has a much smaller time constant in its dynamic behaviour compared to the meter investigated.

The solution which is best available at PTB (due to the other projects we are dealing with) is the establishment of defined flow rates by calibrated sonic nozzles and the flow rate (flow speed) measurement by means of LDV. The general setup for these measurements is given in Fig. 3.

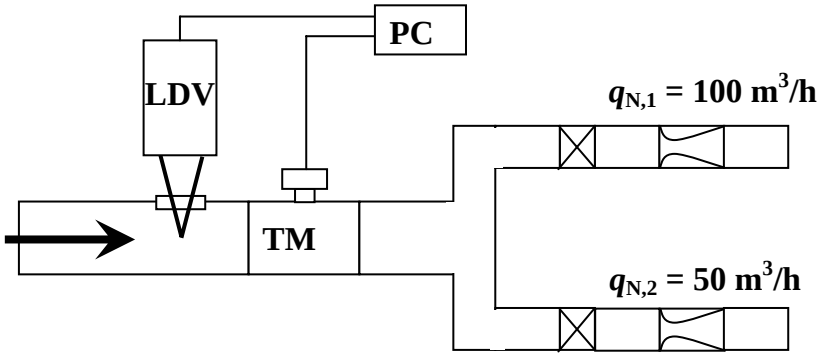

Fig. 3 Experimental setup for low pressure air

The sonic nozzles are operated by pneumatic driven valves, hence the flow rate can be changed quickly by switching different nozzles in the nozzle register. As the nozzles are calibrated, the absolute flow rate at stationary conditions is well known and the flow speed information of the LDV can be calibrated to get directly the actual flow rate within the sampling rate of the LDV indication also under non-stationary conditions. With modern transient recorder equipment, PC technology and sufficient particle seeding one can get sampling rates up to some hundreds per second. Compared to the time constants of some seconds for the mechanical meters under condition of atmospheric air, the time resolution of the LDV indication is absolutely sufficient. Of course also other technologies like hot wire or hot film measurements would fulfil the same purpose. The disadvantage and limiting characteristic of these flow speed measurements at one point of the flow is the relative high variation of the signal due to the turbulence of the flow. Here are potentials for improvements by decreasing the turbulence in the inlet flow by appropriate flow conditioning and the application of multiple sensors for averaging.

[1] Please not that the sign of the parameter C_{TM} has to be considered carefully. In eq. (10) the momentum $M_{fr,D}$ shall have corresponding sign to the difference $q_{TM,ind} - q$.

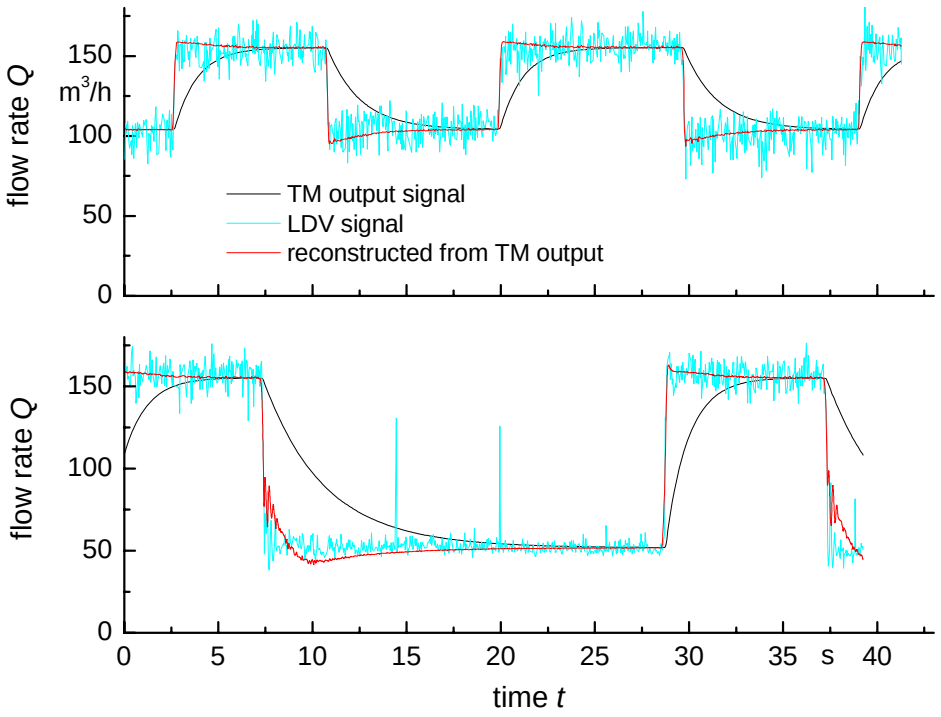

Fig. 4 Measurement results of flow rate indication using the turbine meter and the LDV as well as the reconstructed flow rate based on the indication of turbine meter and the dynamic model eq. (13)

Fig. 4 shows the results of the LDV indicated flow rate, the original indication of the turbine meter as well as the reconstructed flow rate using eq. (13) with the best fitting parameter C_{TM}. and R_m. Best fitting means here the Least Square Approximation of the reconstructed signal to the LDV signal. The parameter R_m in eq. (13) is (as mentioned in chapter 2) a representative mean radius for the location of flow attacking the wheel. In the results of our measurements it came out that it is also a good approach to use a fixed middle value directly derived from the construction with the same quality for the end result.

The two situations shown in Fig. 4, switching from 150 to 100 m^3/h and back as well as from 150 to 50 m^3/h and back, are in first approximation step functions. Corresponding to this, the turbine meter response is similar to an exponential function as one can expect from the differential equation eq. (12) of first order. Looking more detailed to the flow rate indicated by the LDV we find some over speeding of the flow especially when a nozzle is switched of. This caused by the inertia of the flowing gas column and /or by filling/emptying of volumes between the nozzles and the valves. It is impressive how good the reconstructed flow rate also can indicate this behaviour of the real (LDV indicated) flow rate, especially in the case of switching 150 to100 m^3/h. In the case of switching150 to 50 m^3/h the reconstructed flow rate can not represent any longer the real flow rate for extreme slopes but some very typical oscillations of the gas flow shortly after the switch are still visible. The visible limits of the dynamic model acc. eq. (13) is probably caused by the limits in the description for the frictional moment as given in eq. (10). We assume that here is a need of a more detailed and more realistic description for very large differences between the actual angular frequency ω and the virtual frequency ω_0 for stationary condition for the actual

flow rate q (see also note for extrapolation to other fluids below). But for our purposes to find a meter model handling flow variations with in 20 to 30 % we find the situation comfortable.

Note on extrapolation to other fluid conditions: The meter specific parameters R_m (mean radius) and J (inertia of the turbine wheel) in eq. (13) are depending only on the construction of the meter and therefore they are independent to the fluid. In contrary to this, the factor C_{TM} in eq. (10) is depending on the fluid properties and the flow (Reynolds number). To consider this we can express eq. (10) also is following way:

$$M_{fr,\Delta} = C_{TM} \cdot c_P \left(q_{TM,ind} - q\right)^2 \propto \lambda \cdot \rho \cdot \Delta u^2 \tag{14}$$

where λ is the so called friction factor. This friction factor λ is a function of Reynolds number Re with proportionality to $Re^{-0.25}$ for turbulent flows (what we can assume for all of our applications). With the definition of Reynolds number we get:

$$C_{TM} \propto \frac{\rho^{0.75}}{\mu^{0.25}} \cdot \Delta u^{1.75} \tag{15}$$

We made use of the proportionality factor $\rho^{0.75}/\mu^{0.75}$ to transform the factor C_{TM} determined with atmospheric air to high pressure natural gas. The slight difference between the quadratic term for velocity in eq.(10) and the exponent 1.75 in eq. (15) was ignored to keep the possibility of easy transformation of eq. (12) to the explicit solution for the real flow q in eq. (13).

4. Proof under high pressure conditions

After determination of the turbine meter behaviour under low pressure conditions we looked for possibilities to verify the results if applied at the high pressure piston prover (HPPP) which is operated by PTB as the national standard for high pressure gas at the test facility *pigsar*. Outgoing from a short description of the use of the HPPP for calibrations we will explain the use of an ultra sonic meter to check the quality of turbine meter indication correction based on the model determined as described above. A second check will be given by comparison of the calibration results of turbine meters done at different boundary conditions.

It has to be emphasize that we made use of the parameters for eq. (13) as we determined them under atmospheric conditions and their extrapolation for high pressure gas as mentioned in chapter 3. There were not readjustment of the parameters for the high pressure conditions.

4.1 Application of the HPPP using different flow regimes at *pigsar*

Fig. 7 shows an outline of the HPPP. Before the measurement starts , the piston is located at the very left side of the cylinder and the gas flows through the 4-way valve and starting valve S2 (starting valve S1 is closed), then passing the prover run, the 4-way valve and the meter to be tested from where it is returned into the high-pressure grid. The piston is not moved. The measurement is started by simultaneously closing starting valve S2 and opening starting valve S1, thereby allowing gas to flow behind the piston which then starts to move. Piston movement is indicated by switch a1. On passing a2, various impulse and time counters are started and the recording of analogue values (pressures and temperatures) begins. When the piston passes switch

a4, these measurements are stopped. When the piston reaches the end of the piston run, the gas is released through the bypass and the check valve (non-return valve). The use of the HPPP for the calibration of turbine meters is described in detail in [2].

The switch of the gas flow from the pipe via S2 to the pipe via S1 and the acceleration of the piston causes from principle a variation of the actual flow rate. The distance between the location a1 and a2 (fig. 7) is designed to provide enough time for stabilisation of the flow rate, piston speed and the meter indication under normal operation conditions. But the accelerated piston (which has a certain damping friction inside the cylinder) and the two gas columns upstream and downstream to the piston form a complex mechanical system of second order. Depending on the mass of the piston, its friction in the cylinder and the behaviour of the gas columns the characteristic of the piston movement can vary from very strong damped slow acceleration up to high and long lasting oscillations of the piston velocity.

While the mass of the piston and its friction can not be modified in the given system, the two gas columns upstream and downstream to the piston can be varied at *pigsar* in a wide range. Two general possibilities are illustrated in Fig. 5 in the outline of the test facility, the flow regime #1 (red coloured path) and the flow regime #2 (blue coloured path).

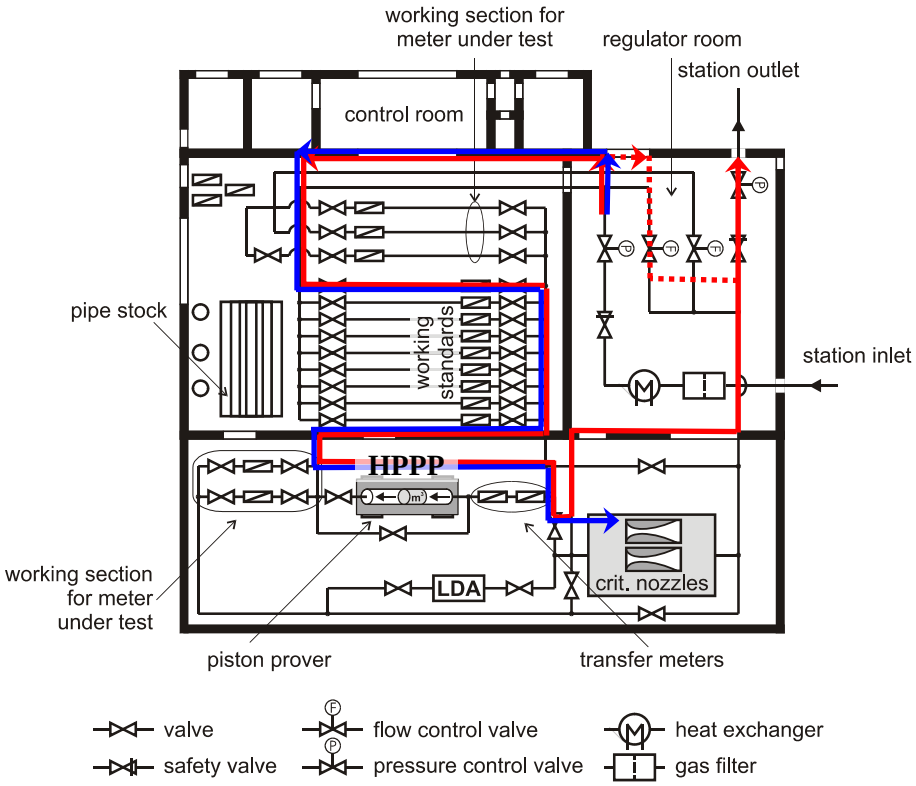

Fig. 5 Outline of pigsar and different flow regimes during use of high pressure piston prover (HPPP) for calibration
flow regime #1, using bypass in regulator station
flow regime #2 via critical nozzles downstream

In the flow regime #1 both gas columns (upstream and downstream the piston of the HPPP) constitute a weak spring. The strength of the upstream column is given due to the use of the bypass in the regulator room and can be varied in wide ranges by means of this. The weakness of

the downstream column is given by the relative large pipe length from the piston to the next pressure/flow regulator at the station outlet.

Compared to this, in the flow regime #2 both gas columns constitute strong (hard) springs. The upstream gas column is characterised by the completely closed bypass. The downstream gas column is kept very short with pipe volume only between the piston and the critical nozzle downstream (the nozzles are something like a wall in this case due to their critical behaviour).

The effect of these two different regimes to the flow rate indicated by the turbine meter during the calibration runs at the HPPP are shown in Fig. 6. While we see a strong variation using flow regime #1 (red curve corresponding to the red coloured flow path in Fig. 5), we find a much better flow rate stability using flow regime #2 (blue curve). The flow rate variation is indicated by the relative change of the actual indication compared to the mean value for the duration of calibration.

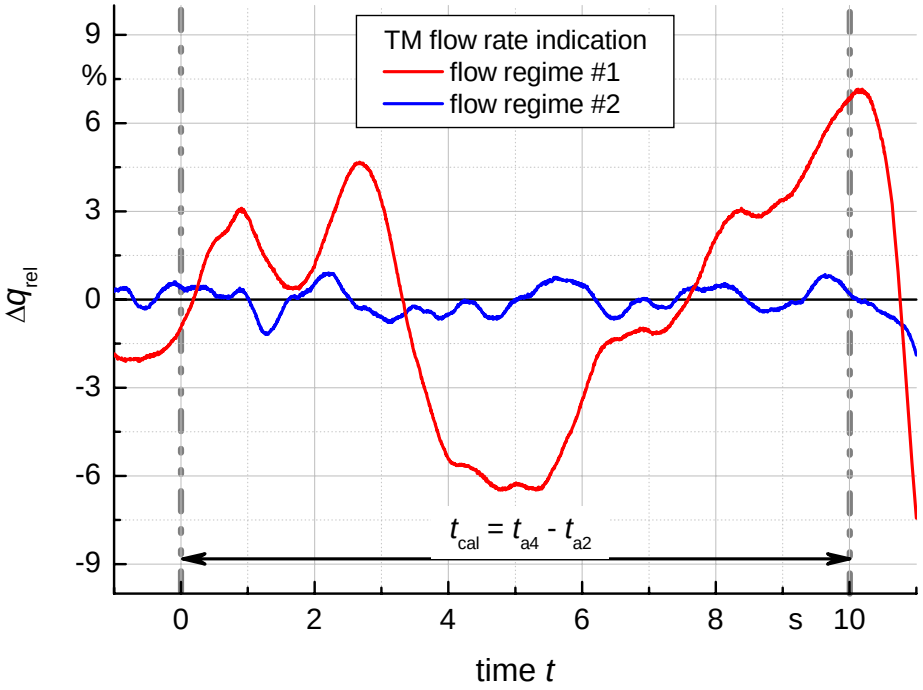

Fig. 6 Example for indication of a turbine meter using different flow regimes at the HPPP
flow regime #1, using bypass in regulator station
flow regime #2 via critical nozzles downstream

4.2 The use of an 8-Path-Ultrasonic meter for fast flow rate indication

Similar to the experiment under atmospheric conditions (chapter 3) we applied a ultra sonic meter (USM) as a second independent meter technology with different dynamic behaviour downstream to the turbine meter as shown in Fig. 7. The USM used for this purpose was an 8-path-USM of the manufacturer Sick-Maihack. Its functionality and general behaviour are described in detail in [4].

From principal, the 8-path-USM consists of two 4-path-meters (path groups A and B) which operate synchronised as one machine. The basic sample time is 40 ms (see also Fig. 8). Every 40

ms the sample schedule for the 4 paths of each group is started. One velocity measurement at one path is done within 5 ms and after further 0.5 ms the measurement at the next path is started. The two groups A and B work hereby simultaneously as outlined in Fig. 8. Therefore we get 4x2 velocity information in sequence within 21.5 ms but in a sample rate of 40ms.

The velocity information of each of the 8 paths lead to flow rate by multiplication with the cross section and a path specific calibration factor. Because this path specific calibration factor would also depend on the specific velocity profile of the installation we make use here of the relative change Δv_{rel} of velocity indication compared to the time average versus the calibration run. This value is then independent to the calibration factor and identical to the relative change of the actual flow rate.

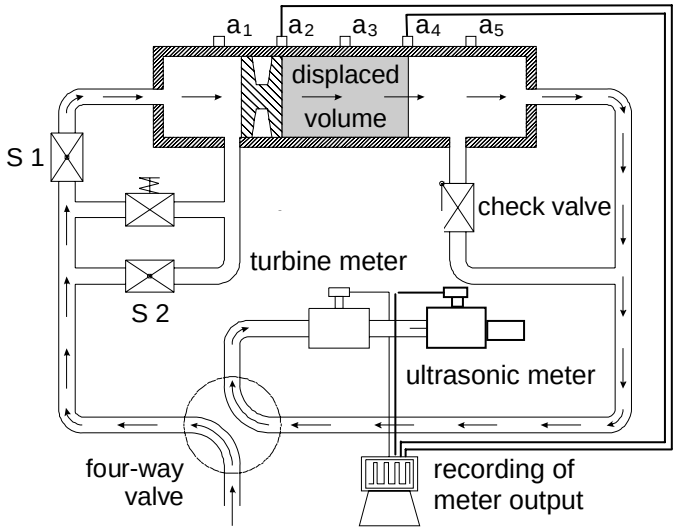

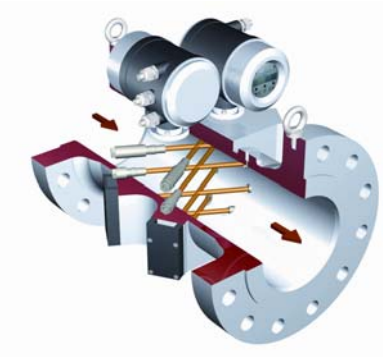

a_1, a_5 : piston position switch
a_2, b_2, c_2 : volume switch (start)
a_3 : volume switch (half range)
a_4, b_4, c_4 : volume switch (stop)

Fig. 7 Outline of HPPP and flow scheme including the turbine meter and the ultrasonic meter

For each basic sample we determined a representative average value out of the 8 paths considering the sampling schedule and the individual time function of indicated relative velocity change of each path by linear interpolation between the sample points.

The synchronisation between the recording of the turbine meter output and the USM indication is done by means of the trigger signals of the HPPP given from the switches a2 and a4 (see Fig. 7). Caused by the properties of the USM logging technology the synchronisation between TM indication and USM indication could not be better than the basis sample time of 40 ms, i.e. a random synchronisation time lag of ±20 ms between both indications.

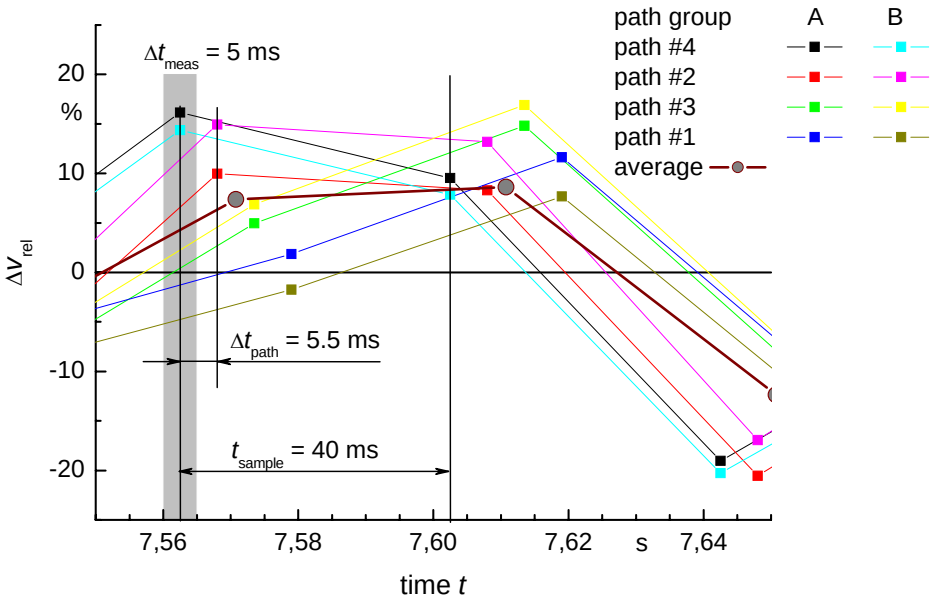

Fig. 8 sampling regime of the 8-path ultra sonic meter (2x4 pathes)

4.3 Test results at high pressure using the ultra sonic meter (USM)

In Fig. 9 the measurement results of relative flow rate change for both the turbine meter (TM) and the USM are shown. Due to the dynamic behaviour of the turbine meter, its indication is damped and delayed compared to the USM signal. But applying the correction for the TM signal according to eq. (13) we get the reconstructed signal which is nearly identical to the USM signal. In the time sale of Fig. 9, the synchronisation time lag of ±20 ms between turbine meter and USM is not visible.

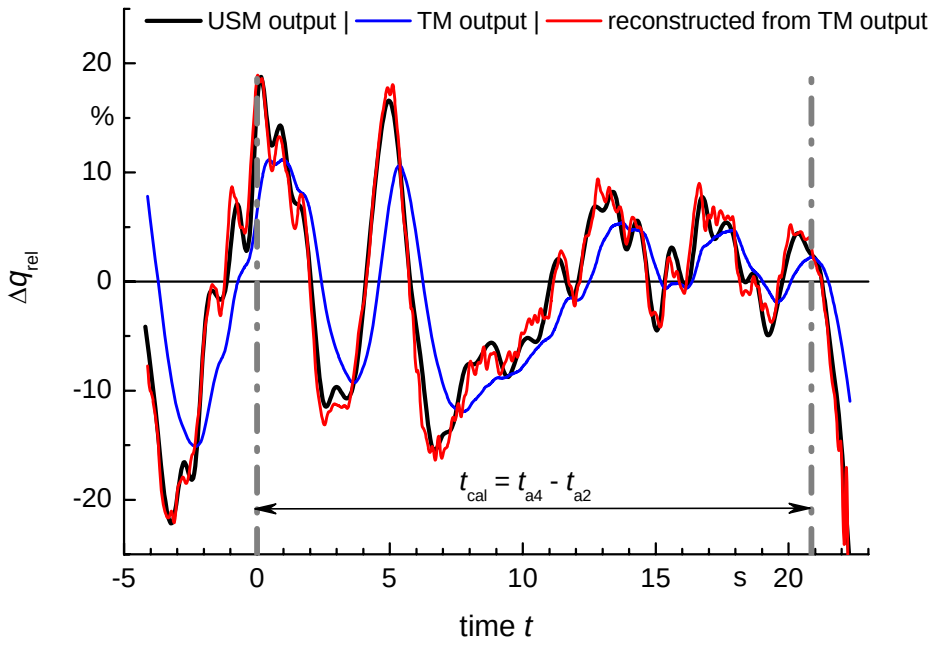

Fig. 9 Measurement results of flow rate changes during a calibration run with high variation of the real flow rate (flow regime #1 in Fig. 5). The measurement was applied at 17 bar and a flow rate of 25 m^3/h.

The next results presented in Fig. 10 are determined in a very special situation at the HPPP which is not in the normal use for calibration but with high potentials to demonstrate the turbine and USM behaviour here. At certain flow rates and pressures the flow through the HPPP system can be quite nice modulated if the piston is located at the end of the piston and the gas has to flow through the checking valve (see Fig. 7). This checking valve is a simple butterfly valve with a small spring to support the valve in closing direction. This spring and the weight of the butterfly wings causes a periodic change of the cross section in these special situation and therefore the modulation of the gas flow rate. The modulation frequency (about 6.5 Hz) is just small enough compared to the sample frequency of the USM (25 Hz) so that we have a sufficient oversampling of the flow rate signal. The original output of the turbine meter is in contrary to this strongly damped and nearly phase shifted by 90°. It can not be used as a representative for the real flow rate changes. But the reconstructed signal by means of eq. (13) is comparable to the USM signal again. In Fig. 10 we show two example of different runs because in this time scale the synchronisation time lag of ±20 ms became important for the interpretation of the result. As one can see in Fig. 10, the reconstructed turbine signal can run by chance 20 ms ahead or after the USM signal. In average over a sufficient number of measurement runs the time shift between both signals is practical zero. This is an impressive demonstration of the abilities of signal reconstruction of the turbine meter output.

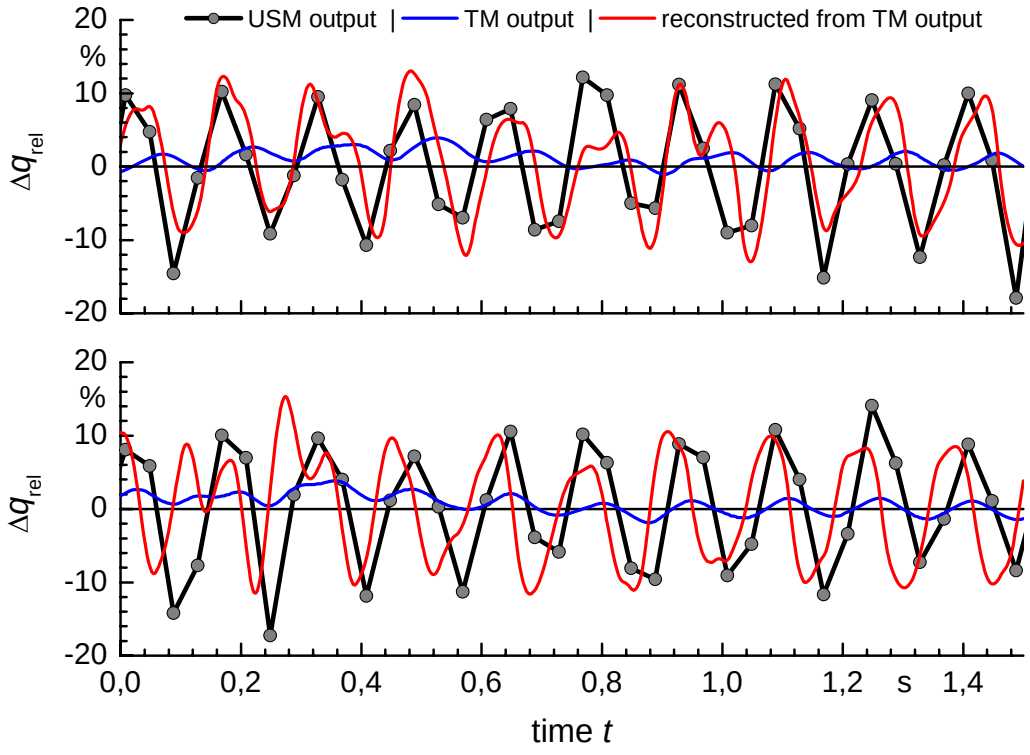

Fig. 10Measurement results for a modulated flow rate at p = 17 bar, q≈ 100 m3/h.

4.4 Application of correction for calibration of turbine meters at HPPP

Finally we like to demonstrate the effect of the output signal correction on the calibration results of the turbine meter using the HPPP. For this purpose we calibrated two turbine meters in series at the HPPP (similar setup as in Fig. 7 but exchange the USM with the second turbine meter). The second turbine meter is the identical type as the first meter and we applied the same values for the parameters in eq. (13) as we found for the first turbine meter without any alteration.

The results of the calibration (i.e. meter deviation) are given in Fig. 11. Again we applied our two basic flow regimes as shown in Fig. 5 (with corresponding colours, red for regime #1 and blue for regime #2). The difference between the calibration results based on the original output (up triangles, solid line rsp.) and the results based on the corrected output (down triangles, dashed-dotted line) is quite high for regime #1 but not for regime #2. Furthermore, in the overlapping part of calibration curves for regime #1 and #2, the results are very consistent only if based on the corrected turbine output. This is valid in similar way for both turbines. With this, the very positive and consistent effect to the calibration results of the turbine meters using the piston prover could be demonstrated.

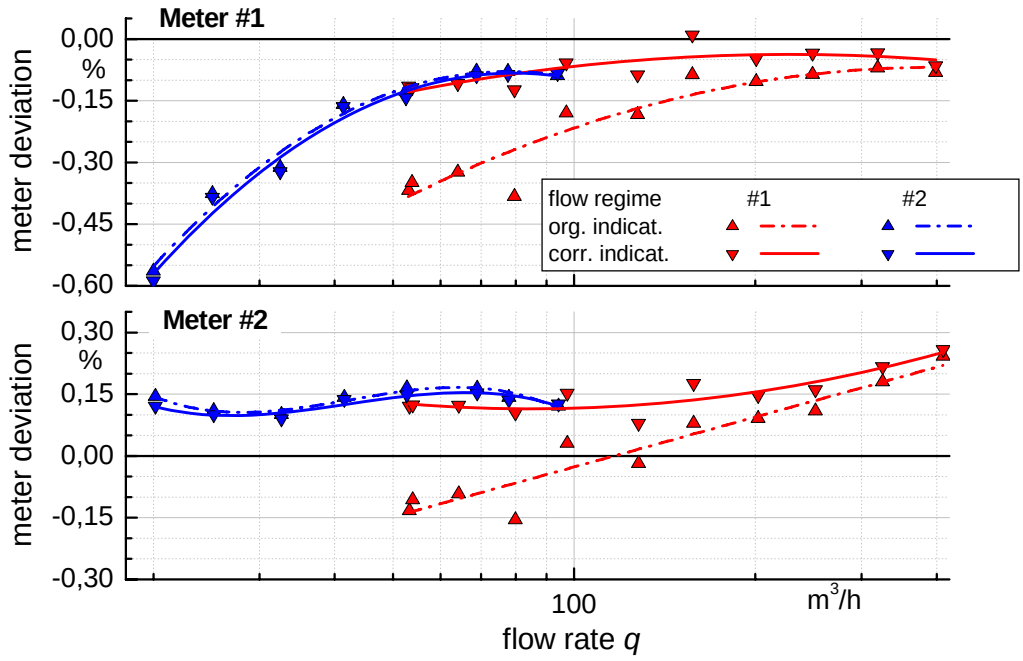

Fig. 11 Example for calibration of two turbine meters using different flow regimes and comparison of meter deviation based on original indication as well as corrected indication. The pressure during calibration was about 17 bar. For flow regime see also Fig. 5.

5. Considerations on uncertainty

The central aim of this investigation was the improvement of the calibration behaviour of turbine meters at the HPPP, especially the support of the figures about uncertainty as already stated in [5]. Therefore we are not interested in a detailed uncertainty analysis of for the reconstructed turbine meter signal. This would be of course possible but rather complex by means of all the information included in the process of parameter determination (chapter 3) and their extrapolation as well as the results of verification under high pressure conditions.

Finally we choose the very pragmatic way to look to the calibration results a shown in Fig. 11 to determine a reasonable empirical uncertainty value of type A for the influence of flow regime. The flow regime #2 is of such quality that there is no impact of the flow variations of more than 0.02%. Furthermore, the calibration results for same flow rate in flow regime #1 and #2 are consistent within ±0.025% (based on the corrected indication for regime #1) even if we apply the parameters of the first turbine meter in eq. (13) for the second turbine without new determination

assuming same values due to the same meter type. For the first meter, the consistency is even better.

Hence, the expanded uncertainty (k = 2) of impact by varying flow rates can be reasonable estimated with 0.025%.

6. Conclusions

The results of investigations documented above allow several conclusions in different directions for the field of dynamic measurements:

- An appropriate dynamic model of a mechanical meter allows the successful correction of the indication to expand the dynamic of this indication. It can become comparable with ultra sonic meters.

- Calibration results based on such corrected output signals are reliable with low uncertainty also for non ideal flow regimes with larger variation of flow rate which can occur especially at piston provers. For turbine meter calibration with the HPPP of PTB we found an uncertainty of 0.025% for this influence.

- The determination of the parameters of the dynamic model can be done at atmospheric air and can be applied then at high pressure conditions.

- The parameters which are specific for the individual meter can be used for meters of the same production series with sufficient results.

- Ultrasonic meters are also good tools for the determination of relative short term variations in the flow rate (but not of the absolute value) within their time resolution of measurement time per path and sampling time. A detailed use of single path information is necessary.

The results documented in this paper will get also high importance especially due to the fact that nowadays new primary standards for the unit for volume of high pressure gas are introduced which are also based on piston prover technology. Hence, we need this more detailed knowledge to avoid misinterpretation of inter comparison results between such facilities of similar technology in the future. Consequently, the investigation of the behaviour of rotary meters is will be also a task under same topic because this technology is also commonly used as secondary and transfer standard.

7. Symbols

Table 1 Symbols

symbol	description
J	moment of inertia of the turbine wheel
q	(real) volume flow rate
$q_{TM,ind}$	flow rate, indicated by turbine meter
$\dot{q}_{TM,ind}$	first derivative of indicated flow rate
Δq_{rel}	Relative change of flow rate compared to an average value (time average)

ρ	density
μ	dynamic viscosity
R_m	mean radius of turbine wheel
A	Cross section of turbine wheel
$\tan\beta$	blade angle of turbine wheel
M_{drive}	driving torque caused by flow at the turbine wheel
M_{fr}	torque caused by friction forces
$M_{fr,0}$	(friction) torque at stationary condition $\omega = \omega_0$
$M_{fr,\Delta}$	additional (friction) torque at non stationary conditions $\omega \neq \omega_0$
C_{TM}	parameter of turbine characteristic
c_P	calibration factor of turbine meter (pulse factor)
u	Axial flow velocity at turbine wheel
Δu	velocity difference driving the turbine wheel
ω	actual angular frequency of the turbine wheel
$\dot{\omega}$	first derivative of actual angular frequency
ω_0	angular frequency of the turbine wheel at stationary condition

8. References

[1] Technische Richtlinien der PTB - Messgeräte für Gas
G 13:Einbau und Betrieb von Turbinenradgaszählern (03/02)

[2] B. Mickan, R. Kramer, H. J. Hotze, D. Dopheide: "PIGSAR - The Extendet Test Facility and New German National Primary Standard for High Pressure Natural Gas", Conference Proceedings, 5th International Symposium on Fluid Flow Measurement (ISFFM), Arlington, USA, 7-10 April 2002, CD-ROM, Session 17, p. 1-20

[3] J. Bergervoet, M.M.W. van Wezel, Neues Diagnoseverfahren für eingebaute Turbinenradzählern; 3. KÖTTER Workshop Gasmengenmessung, Rheine, 2008

[4] V. Herrmann, M. Wehmeier, T. Dietz, R. Kramer, B. Mickan: A new low pressure calibration facility using 8-path-ultrasonic meters as working standards; Conference Proceedings, 6th International Symposium on Fluid Flow Measurement (ISFFM), Queretaro, Mexico, May 16-18 2006

[5] B. Mickan, R. Kramer, D. Vieth, H.-M. Hinze, The Actual Results of Recalibration and Improvements of the Traceability Chain as well as the Uncertainty for Measurement in High Pressure Natural Gas in Germany, Proceeding of the 14th Flomeko 2007, Johannesburg, South Africa, Sept. 19th – 21st 2007